AFRL-VS-HA-TR-98-0013

GPS SCINTILLATION ANALYSIS

Ronald G. Caton
Michael J. Kendra
William J. McNeil

Radex, Inc.
Three Preston Court
Bedford, MA 01730

January 15, 1998

Scientific Report #6

Approved for public release; distribution unlimited

AIR FORCE RESEARCH LABORATORY
Space Vehicles Directorate
29 Randolph Road
AIR FORCE MATERIEL COMMAND
HANSCOM AIR FORCE BASE, MA 01731-3010

This Technical Report has been reviewed and is approved for publication"

John Cipar

JOHN CIPAR
Contract Manager

LT COL FRANK ZAWADA
Branch Chief

This report has been reviewed by the ESC Public Affairs Office (PA) and is releasable to the National Technical Information Service (NTIS).

Qualified requestors may obtain additional copies from the Defense Technical Information Center (DTIC). All others should apply to the National Technical Information Service (NTIS).

If your address has changed, if you wish to be removed from the mailing list, of if the address is no longer employed by your organization, please notify PL/IM, 29 Randolph Road, Hanscom AFB, MA 01731-3010. This will assist us in maintaining a current mailing list.

Do not return copies of this report unless contractual obligations or notices on a specific document require that it be returned.

REPORT DOCUMENTATION PAGE

Form Approved
OMB No. 0704-0188

1. AGENCY USE ONLY *(Leave Blank)*	2. REPORT DATE	3. REPORT TYPE AND DATES COVERED
	15 January 1998	Scientific Report No. 6

4. TITLE AND SUBTITLE

GPS Scintillation Analysis

5. FUNDING NUMBERS

PE 63871 C
PR 7659 TA GY WU AG
Contract F19629-95-C-0106

6. AUTHORS

Ronald G. Caton
Michael J. Kendra
William J. McNeil

7. PERFORMING ORGANIZATION NAME(S) AND ADDRESS(ES)

Radex, Inc.
Three Preston Court
Bedford, MA 01730

8. PERFORMING ORGANIZATION REPORT NUMBER

RXR-980101

9. SPONSORING / MONITORING AGENCY NAME(S) AND ADDRESS(ES)

Air Force Research Laboratory
29 Randolph Road
Hanscom AFB, MA 01731-3010
Contract Manager: John Cipar/VSSW

10. SPONSORING / MONITORING AGENCY REPORT NUMBER

AFRL-VS-HA-TR-98-0013

11. SUPPLEMENTARY NOTES

12a. DISTRIBUTION / AVAILABILITY STATEMENT

Approved for Public Release
Distribution Unlimited

12b. DISTRIBUTION CODE

13. ABSTRACT *(Maximum 200 words)*

Scintillation data recorded by Global Positioning System (GPS) receivers in various locations are examined. This report details our investigation into the validation of the GPS S_4 and 60-second phase sigma values for their inclusion into the Air Force Research Laboratory Scintillation Network Decision Aid (SCINDA) as an aid in issuing L-band scintillation warnings and predictions. GOES8 L-band data is compared with GPS S_4 and phase sigma levels during moderate scintillation. The construction of and need for site specific masks to reduce the possibility of issuing false scintillation warnings due to persistent anomalous spikes seen in the GPS data, likely due to multipath interference, is also discussed.

14. SUBJECT TERMS

GPS, Global positioning system, Scintillation, L-band, S_4, Phase sigma, Ionospheric disturbances, SCINDA, Multipath, Masks, NovAtel, 630 nm all-sky images, Ionospheric depletions, Paq communications

15. NUMBER OF PAGES

34

16. PRICE CODE

17. SECURITY CLASSIFICATION OF REPORT	18. SECURITY CLASSIFICATION OF THIS PAGE	19. SECURITY CLASSIFICATION OF ABSTRACT	20. LIMITATION OF ABSTRACT
Unclassified	Unclassified	Unclassified	Unlimited

NSN 7540-01-280-5500

Standard Form 298 (Rev. 2-89)
Prescribed by ANSI Std. Z39-1
298-102

TABLE OF CONTENTS

LIST OF FIGURES

ACKNOWLEDGEMENTS

The authors wish to acknowledge the contributions of Santimay Basu, Keith Groves, Capt. Matt Smitham, and Ed Weber of AFRL/VSBI, and Peter Ning of KEO Consultants in preparing this report. Cesar Valladares of AFRL/VSBI and Bob Livingston of SRI International are responsible for the data collection at Ancón and Antofagasta, respectively. The 630 nm all-sky data and GPS signal-to-noise from Ascension Island on 1 October 1994 were made available by Ed Weber. Anthony Long of Radex, Inc. is primarily responsible for SCINDA visualization.

LIST OF ACRONYMS

AFB	Air Force Base
AFRL	Air Force Research Laboratory
ASCII	American Standard Code for Information Interchange
GPS	Global Positioning System
GPSI	Ionospheric Effects Branch (now VSBI)
GPSM	Space Operational Models Branch (now VSBP)
GUI	Graphic User Interface
IDL	Interactive Data Language, a graphics software package
PC	Personal Computer
PL	Phillips Laboratory (now AFRL/VS)
PL-SCINDA	Phillips Laboratory Scintillation Network Decision Aid
PRN	Psuedorandom Noise
SGI	Silicon Graphics, Incorporated
SNR	Signal to Noise Ratio
SV	Space Vehicle
TEC	Total Electron Content
UHF	Ultra High Frequency
UT	Universal Time
VS	Space Vehicles Directorate (AFRL)
VSBI	Ionospheric Effects Branch of AFRL/VS

1. INTRODUCTION

The global coverage provided by the Global Positioning System (GPS) constellation, along with the availability of receivers, has greatly enhanced our ability to examine the ionosphere. Several recent ionospheric studies have benefited greatly from the use of GPS data, such as, studies of ionospheric perturbations [*Ho, et al.,*1996; *Calais and Minster,* 1996], ionospheric total electron content [*e.g. Pi, et al.,* 1997; *Beach, et al., 1997*], and upper frequency limit (f_oF_2) predictions for HF propagation [*Houminer and Soicher,* 1996]. This report details our investigation of scintillation data recorded with modified NovAtel GPStation receivers located at Antofagasta, Chile, Ancón, Peru, and here at Hanscom Air Force Base in Bedford, Massachusetts. The units positioned in Chile, Peru, and other regions of military importance, are to become part of the Air Force Research Laboratory (formerly Phillips Laboratory) Scintillation Network Decision Aid (SCINDA) [*McNeil, et al.*, 1997], which provides L-band, as well as UHF, scintillation warnings. Several important issues, including multipath effects and a comparison of GPS measurements with GOES8 L-band scintillation data, are discussed.

2. GPS COMPARISON WITH ALL-SKY IMAGES OVER AGUA VERDE, CHILE

As an initial study of the validity of using GPS data to detect ionospheric disturbances, comparisons were made with a data set containing reconstructed eastward and westward edges of four ionospheric depletion bands seen in 630 nm airglow images over Agua Verde, Chile. This data, collected during the evening of October 1, 1994, spanned two hours beginning at 00:00 UT. GPS signal-to-noise ratio (SNR) and total electron content (TEC) measurements from Agua Verde were also provided. In Figure 1, the depletion regions are shown in 10 minute time steps as gray shaded areas. The ionospheric penetration points of the GPS satellites at 300 km are included as solid circles for satellites above a selected minimum elevation angle. They are shaded either light gray ("not scintillating") or black ("scintillating"). The two independent systems agree quite well when considering the geometrical effects of locating the precise bubble edges.

Several steps were involved in producing the image in Figure 1. First, the eastward edge of one of the four reconstructed depletions, which originally contained only a westward edge between 01:30 and 02:00 UT, was extended to 02:00 UT. This was accomplished by computing the average longitudinal extension of the bubble prior to 01:30 UT and calculating the appropriate values to fill the region. The extended area is shown in light gray in Figure 2 where the longitudinal extent of all four bubbles are shown versus the Universal Time.

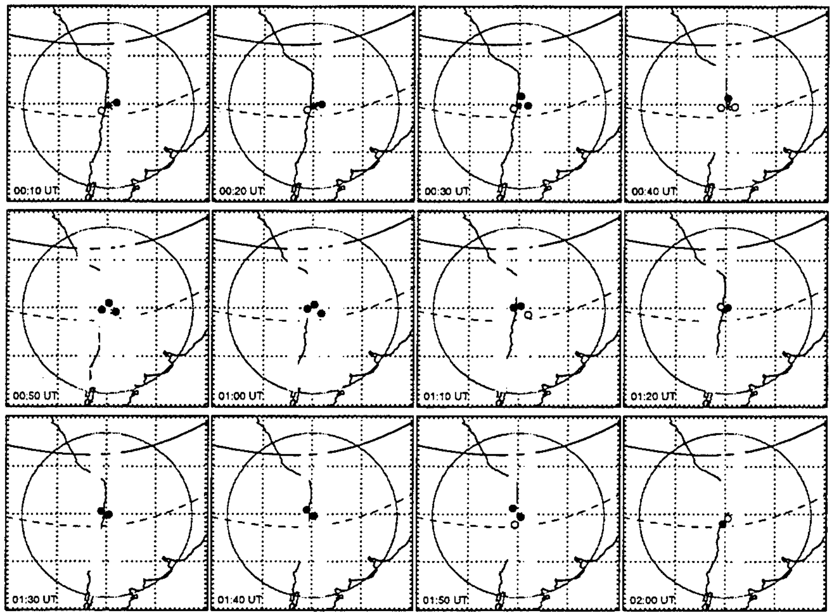

Figure 1. Airglow depletions and GPS scintillation levels from 1 October 1994. 630 nm All-Sky depletions are displayed as gray shaded areas. GPS S_4 levels for satellites above 50° elevation are shown as colored circles with gray, indicating no scintillation, and black, indicating scintillation exceeding the chosen threshold of 0.1. The location of the imager at Agua Verde (25.4° South, 69.9° West) is displayed as an asterisk. Latitude and Longitude grid lines are shown in 10° increments. The magnetic equator is labeled with a solid line while the dotted line represents the area 15° from the magnetic equator usually associated with the equatorial anomaly.

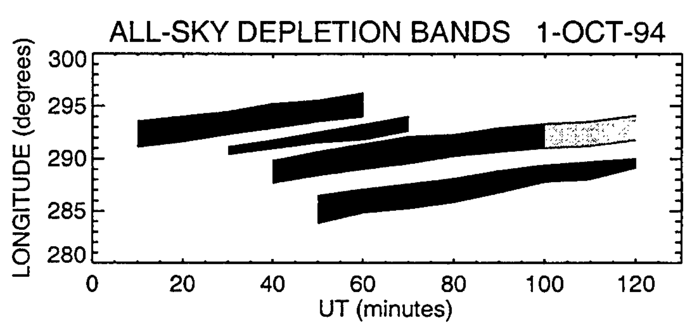

Figure 2. Longitudinal Extensions of All-Sky Depletions from 1 October 1994.

Next, the ephemeris of each GPS satellite was generated from the appropriate orbital elements. The ionospheric penetration points, along the line to Agua Verde, were then calculated assuming a penetration point at 300 km. Because we were interested in S_4 levels, we computed an S_4 value from the signal-to-noise ratio (SNR) using 5-minute averages to be consistent with SCINDA computations. S_4 values were calculated using the following equation from *Aarons and Basu* [1985]:

$$(S_4)^2 = \frac{\langle P^2 \rangle - \langle P \rangle^2}{\langle P \rangle^2}$$

Where P is defined as the power in dB. Because raw power was not included in the data set, the SNR values were used with the following equation defining P as:

$$SNR = 10\log_{10}[P]$$

or

$$P = 10^{\frac{SNR}{10}}$$

Because the reconstructed depletion band edges from the all-sky data were available in 10-minute intervals, the 5-minute average S_4 values were converted to 10-minute averages.

Weber, et al. [1996] suggested that a peak-to-peak fluctuation in the SNR of 7 dB, commonly seen in the 1 October 1994 data from GPS space vehicles (SV) 21, 22, and 23, corresponds to an S_4 index of approximately 0.35. Our values, shown in Figure 3 tend to agree with this, producing values of approximately 0.3 for GPS satellite number 21 during the heaviest scintillation. These numbers may be slightly lower than suggested by *Weber, et al.* [1996], although they are consistently calculated, and allow us to distinguish relative scintillation levels over time.

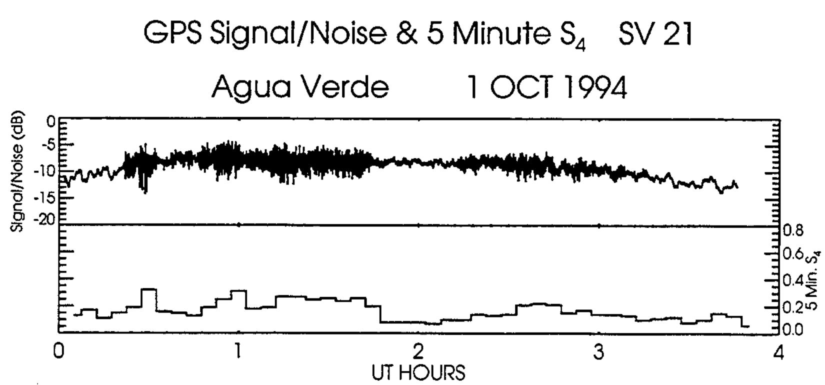

Figure 3. GPS data from Agua Verde, Chile on the night of 1 October 1994. Signal/Noise measurements were used to calculate S_4 values using equations 1 through 3. During the maximum scintillation seen near 01:30 UT, our S_4 levels of approximately 0.3 compare favorably with the levels in *Weber, et al.* [1996].

3. SYSTEM DESCRIPTION

In order to collect ionospheric scintillation data from the GPS constellation, several NovAtel GPStation receivers have been modified by Paq Communications, in Milpitas, California, with software to track up to eleven GPS satellites at L1 frequency (1575.420 MHz) while measuring and recording both phase and amplitude scintillation. This data, along with additionally selected logs, such as the receiver position and the raw data (collected at 50 Hz) used for scintillation calculations, is stored in hourly binary files. The scintillation logs, named ISMR, are produced at the top of each minute and include the azimuth, elevation, S_4, a correction to S_4, and phase sigma measurements for each GPS satellite in view. The satellites are identified by their Pseudo-Random Noise (PRN) or Space Vehicle (SV) numbers.

The system currently in place, ultimately displaying the GPS scintillation data with the Scintillation Network Decision Aid software (SCINDA) [*McNeil, et al.*, 1997], is configured as follows. A PC configured with a Linux operating system at the receiver sites, currently operational in Antofagasta, Chile, and Ancón, Peru, records the most recent position and scintillation information in files named "latest.pos" and "latest.ismr" every sixty seconds. This data is also appended to a larger file including all data collected over the last sixty minutes. The data in this hourly file is limited to the date, time, satellite number, and scintillation data (either 60-second phase sigma or S_4) in order to reduce bandwidth during the data transfer to AFRL that takes place every 15 minutes. Here, the files are edited and written to nightly data files containing the GPS position and scintillation data in 60 second intervals. These raw files are then processed a second time with a masking routine designed to reduce the errors induced by suspected multipath interference in the GPS signal The masking is described in a separate section of this report. An averaging process is then applied producing the final nightly 5-minute averaged masked files which are fed to SCINDA and displayed on the screen. The 300 km ionospheric penetration point of each GPS satellite is represented in SCINDA as a 3-dimensional sphere colored to distinguish levels of scintillation. A SCINDA L-band display is shown in Figure 4. GPS penetration points are shown for the eight visible satellites from Antofagasta, Chile at 03:45:00 UT on 12 September 1997 and shaded according to their scintillation level. A green sphere indicates a pure GPS signal while yellow and red, respectively, represent a moderate or severe L-band disruption due to equatorial ionospheric plumes.

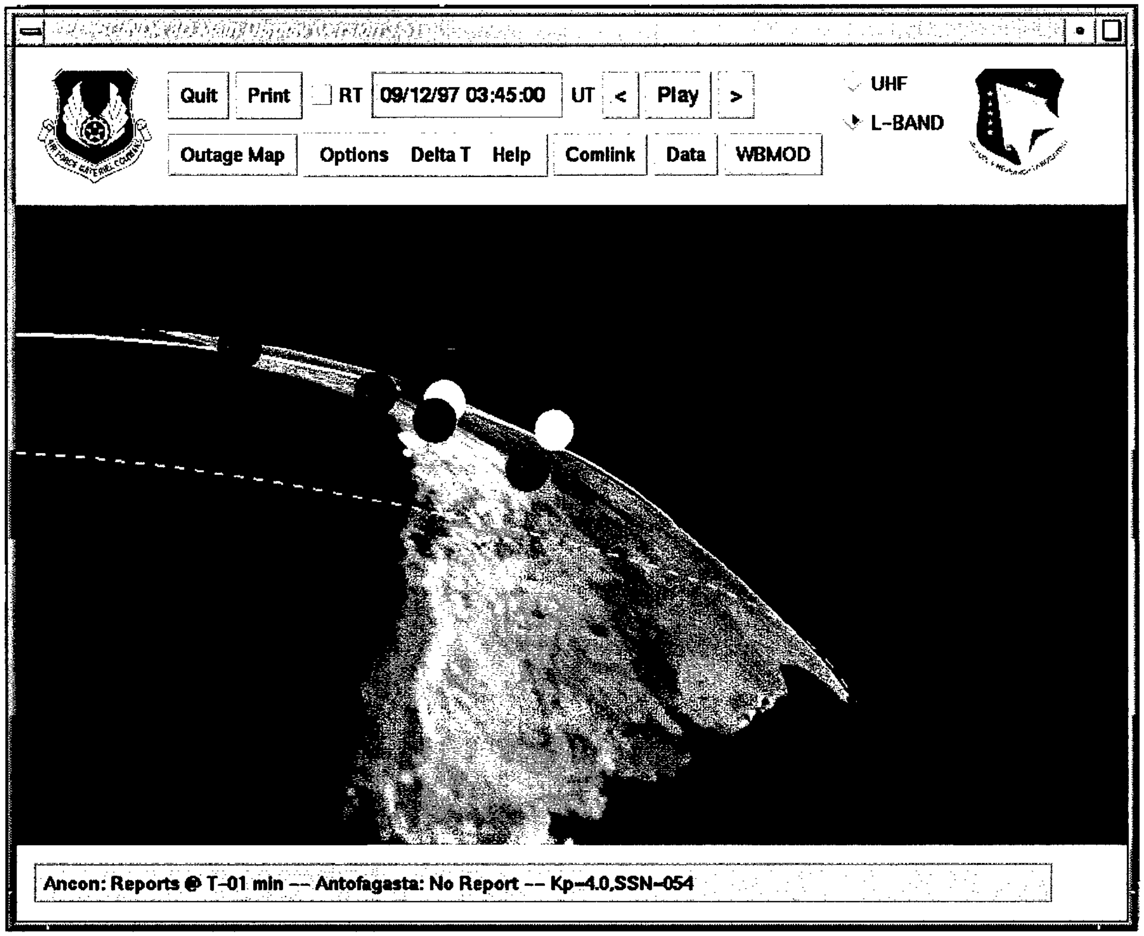

Figure 4. SCINDA display of GPS ionospheric penetration points over Antofagasta, Chile from 12 September 1997 at 03:45:00 UT. The 300 km penetration points are represented by spheres and colored to indicate the level of signal disturbance along the comlink. A green sphere signifies no scintillation while yellow and red, respectively, represent moderate and severe disturbances.

4. SOFTWARE

Various processing and tracking programs were written for signal validation studies of the GPS scintillation data collected by the NovAtel receivers before incorporating the L-band capabilities into SCINDA. The first of these routines were designed for processing the binary files available from the Paq Communications software on the NovAtel receivers. Separate routines were developed for extracting the information for the individual data logs (ISMR, SIN, DIV, and POS) from the hourly binary data files to ASCII files for future examination. The hourly ASCII files were then combined into daily and nightly files for archival purposes and the scintillation data was plotted and analyzed. An example of a nightly summary plot from a comparatively inactive day for

L-band disturbances over Antofagasta, Chile is shown in Figure 5. Here the GPS S_4 values are plotted, along with the elevation angles, as a function of the universal time for five individual satellites visible on the evening of 23 November 1996 (96328). Elevation angle slowly increases to a maximum value then decreases as the GPS satellite rises and sets with respect to the site, making it easy to distinguish from the S_4 data also shown in each plot. The UHF S_4 values measured at Antofagasta during this time, from a link to Fleetsat8, indicate only moderate scintillation, not detectable in the L-band.

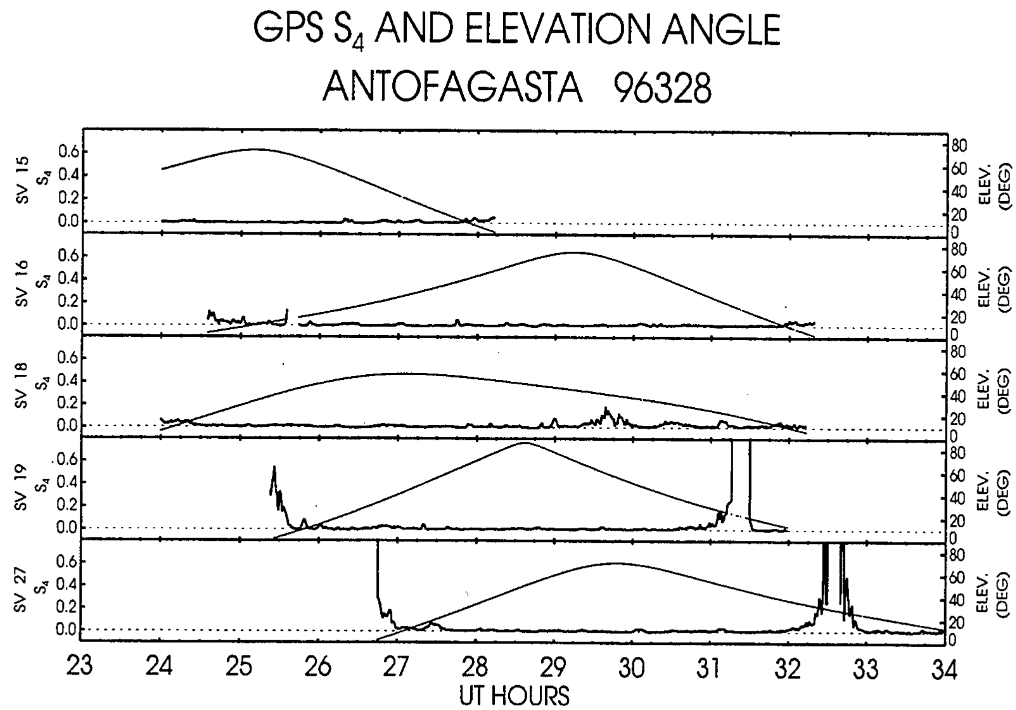

Figure 5. S_4 and elevation angles for selected GPS satellites from the NovAtel receiver at Antofagasta on the evening of 23 November 1996 (96328).

Large S_4 values, as seen in Figure 5 for SV 19 at low elevation angles, are often, but not always, seen near the horizon due to signal loss. The S_4 spikes seen in SV 19 just after 31:00 UT and SV 27 just before 33:00 UT, which correspond to 07:00 UT and 09:00 UT on the following day, are likely due to multipath interference and will be discussed in more detail in the following section on signal validation. It should be noted that because the binary files were written on a PC, the FORTRAN programs written for processing these NovAtel files may not be run in the SUN or SGI environments without a routine to reorder the bytes. It should also be pointed out that an error was noticed in the exact order of the bytes in the binary ISMR log, as given in Table IV of the <u>Ionospheric Scintillation Monitor User's Manual Draft</u> [*Hua*, 1996]. The "receiver status" and "Number of SV observations" fields have been reversed.

In analyzing the summary S_4 and elevation angle plots, it was noticed that for certain GPS satellites, increases in S_4 are repeatedly seen, from orbit to orbit. Two such examples are evident in Figure 5 for satellites 19 and 27 at 31:30 and 32:30 UT, respectively. For another look at this, see Figure 6, where S_4 values from SV 27, over Antofagasta, are shown for five consecutive evenings. Notice that in each case, the S_4 values recorded near 32:30 UT are extremely large. To examine this, a Graphic User Interface (GUI) was developed to allow a user to choose from a selection of all available GPS satellites and plot the satellite tracks over a period of time. The visual interface for this program is shown Figure 7. Here, 300 km ionospheric penetration points above Antofagasta, Chile, for five GPS satellites are displayed from 30:30 to 32:00 UT along with elevation angle contours at 30 and 90 degrees. Penetration point positions at 32:00 UT are indicated by symbols for each individual satellite. Notice that at 32:00 UT, SV 27, the filled diamond, is located in nearly the identical position as SV 19, the filled triangle, at 31:00 UT. This region of the sky to the southwest of Antofagasta is clearly affected by interference which depends only on satellite position. We suspect that this interference is due to multipath effects.

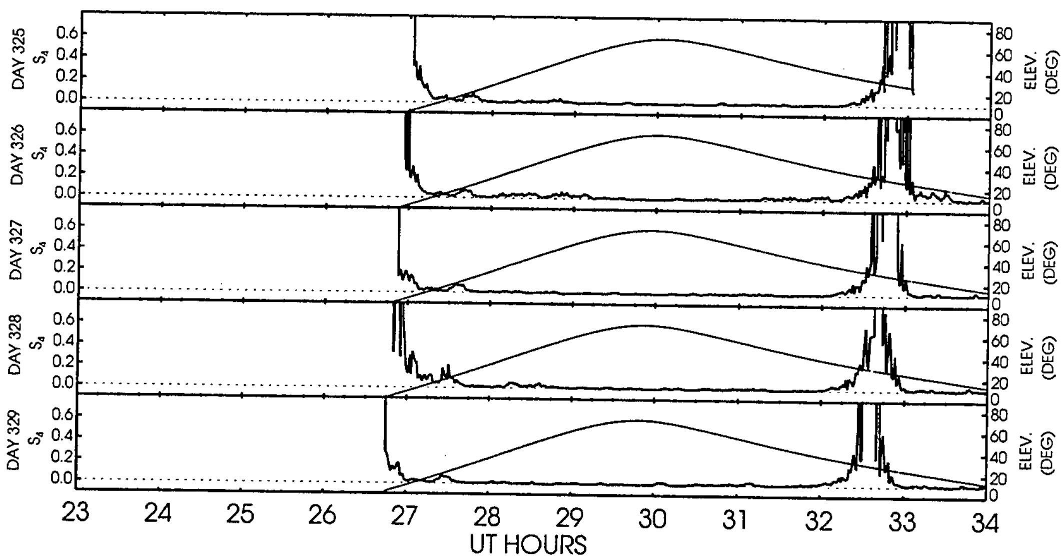

Figure 6. GPS S_4 and elevation angles over Antofagasta, Chile are shown for SV 27 for five consecutive evenings. The persistent spike in the S_4 measurements near 32:30 UT each night are due to a location specific signal interference, most likely due to multipath effects.

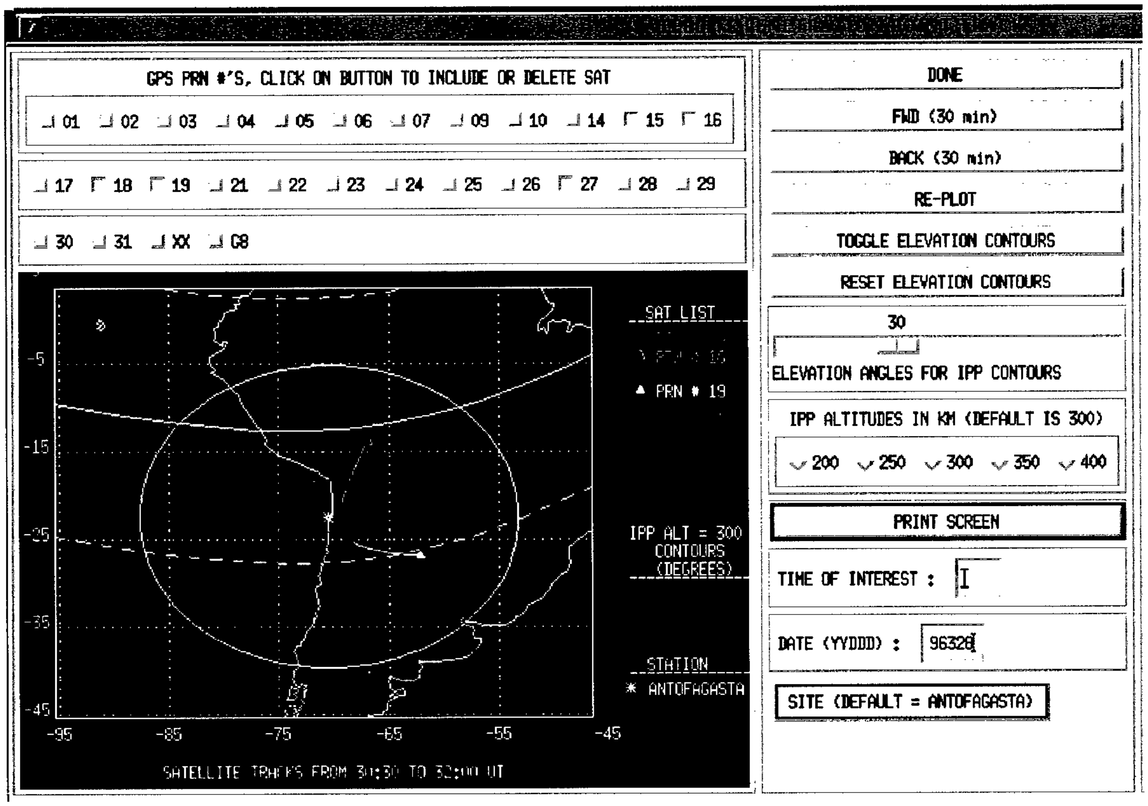

Figure 7. View of the Graphic User Interface (GUI) used to determine satellite ionospheric penetration point positions. Various sites (Antofagasta, Agua Verde, and Ancón) may be chosen for the receiver location. Elevation angle contours are selected with the slider while satellites are chosen with the click of the buttons located on the top panel. Satellite tracks, with the various colored symbols at the head, are displayed for the past one and one half hours from time specified at on the bottom of the screen.

The anomalous interference seen in the GPS signals from Antofagasta is also present in data collected from other sites. Because of this, a characterization of each individual antenna configuration is essential. In order to investigate these effects, programs were developed to process the scintillation files from each site, averaging the S_4, 60-second phase sigma, and carrier-to-noise data in one degree azimuth and elevation angle bins, with an attempt to exclude real scintillation. Because the entire data set was collected near solar minimum conditions, very little L-band scintillation was seen. The resulting files from this averaging process were plotted with an IDL routine highlighting the distinct differences between the antenna configurations at Antofagasta, Chile and Ancón, Peru. The average Carrier/Noise (dB-Hz) values from Ancón and Antofagasta are shown in Figure 8. The use of figures similar to these in developing site specific GPS masks to minimize the effects of persistent interference will be discussed further in Section 6 (Antenna Pattern Characterization) of this report.

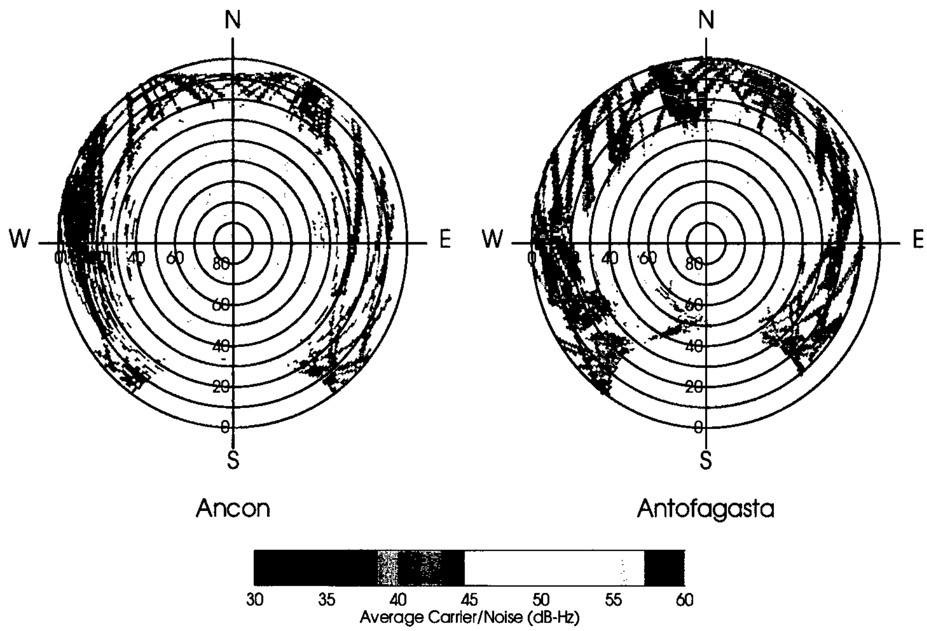

Figure 8. GPS average Carrier/Noise values in one degree azimuth and elevation bins from Ancón, Peru and Antofagasta, Chile. Ancón data was collected between 15 November 1996 (96320) and 24 January 1997 (97024). Antofagasta data collected from 28 October 1996 (96302) to 13 June 1997 (97164). Each set contains frequent data dropouts.

5. SIGNAL VALIDATION

Before incorporating GPS data into SCINDA, it was necessary to validate the L-band S_4 values recorded by the modified NovAtel receivers. To accomplish this, raw power and phase measurements at 50 Hz were to be recorded for comparison with the one-minute ISMR logs containing S_4 values. Processing of the binary logs collected during a campaign at Nyalesund indicated that a bug in the software prevented the recording of the raw data. This problem was corrected after contact with Quyen Hua of Paq Communications and a second attempt at recording raw data was made during campaign at Ascencion Island. Once again, this was unsuccessful. Although raw power and phase values were recorded, the software had been configured to store high frequency data for each satellite in view. Due to the limitations of the system, this led to large gaps in the raw data making any S_4 computations impractical. Following this, two NovAtel receivers were set up at Radex for local data collection and evaluation. Raw power and phase data were collected, along with the one-minute S_4 logs, for up to three GPS satellites at a time, while artificially disrupting the signal. Data sets were compiled for zero, moderate and heavy interference. The raw data was processed and made available for further processing and comparison with the S_4 levels registered by the Paq Communications software in the NovAtel GPS receiver. It was reported that the recorded S_4 levels were, at times, extremely high, especially during periods of intense interference. This problem is currently under investigation with the use of equipment at Wright-Patterson AFB for inducing specified levels of disturbance to the signal.

After processing more than one thousand hourly binary files from Antofagasta, Chile and Ancón, Peru, the hourly files were combined into nightly files and summary S_4plots were produced. An example, from the 'quiet' evening of 96328, is shown Figure 9. Comparing the S_4 values on 96328 with those measured 96325 (Figure 10), notice that a very weak scintillation event was detected by GPS satellites 15, 18, and 19 near 26:00 UT. Because the S_4 spikes seen in the both Figures 9 and 10 for SV 19 near 31:00 UT , and SV 27 near 27:00 UT and 33:00 UT are repeatedly seen for each orbit, they can not be considered real scintillation. More likely, they are the result of multipath interference. The same explanation may apply for the large S_4 measurements at low elevation angles for nearly all of the satellites. This becomes an extremely important issue when using this data for issuing scintillation warnings and is addressed in Section 6 of this report.

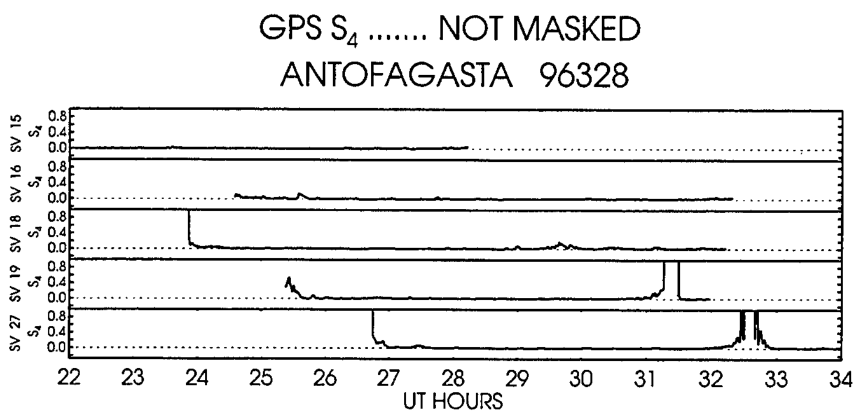

Figure 9. GPS S_4 values recorded for selected satellites over Antofagasta on the eveniing of 23 November 1996 (96328).

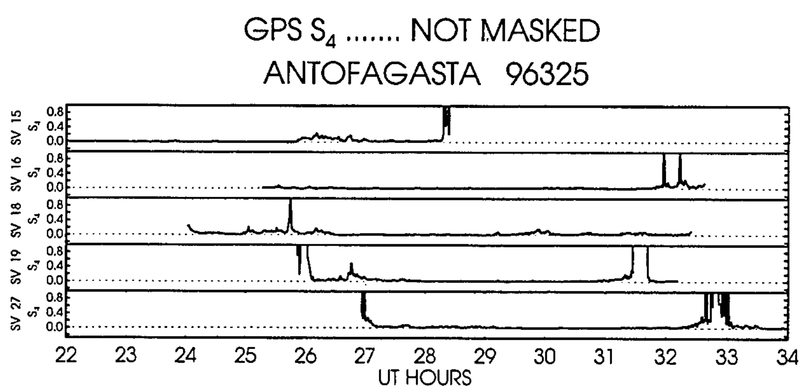

Figure 10. GPS S_4 values recorded for selected satellites over Antofagasta on the evening of 20 November 1996 (96325). Very moderate scintillation was measured on this night.

The scintillation event seen in Figure 10 from 25:00 UT to 27:00 UT, although not extremely strong, is rarely seen in the data collected at the time of this writing. Because the GPS receivers were installed at both South American locations during the solar minimum conditions of 1996, the amount of L-band scintillation detected was expected to be quite minimal. As the solar cycle ramps up in the coming years, it is believed that this activity will significantly increase [*Bishop,* 1994]. The scintillation event shown in Figure 11 is an indication that this has already begun to occur. Substantial scintillation is seen in the NovAtel data from the evening of 21 April 1997 (97111) near 25:00 UT. L-band scintillation was observed by each of the satellites included in this figure, as well as GOES8 (see Figure 12), a geosynchronous satellite located almost directly over Antofagasta, Chile. On the night of 21 April 1997 (97111), scintillation levels from the GOES8 satellite, broadcasting in the L-band at 1685 MHz, were measured between 0.2 and 0.4 for approximately two hours near 25:00 UT. Because S_4 is frequency dependent, direct comparisons between measurements at extremely different frequencies cannot be made. For example, UHF scintillation on the Antofagasta link to Fleetsat8 at 250 MHz during this same time period measured in the range of 0.8 to 10.0. However, because the GPS satellites are broadcasting at a frequency of 1575.42 MHz, S_4 comparisons with GOES8 (at 1685 MHz) are relevant. In comparing Figures 11 and 12, it is obvious that the S_4 levels recorded by the NovAtel receivers during this event were much too high. This apparent problem has been duplicated in the subsequent examinations of the receivers detailed earlier in this section.

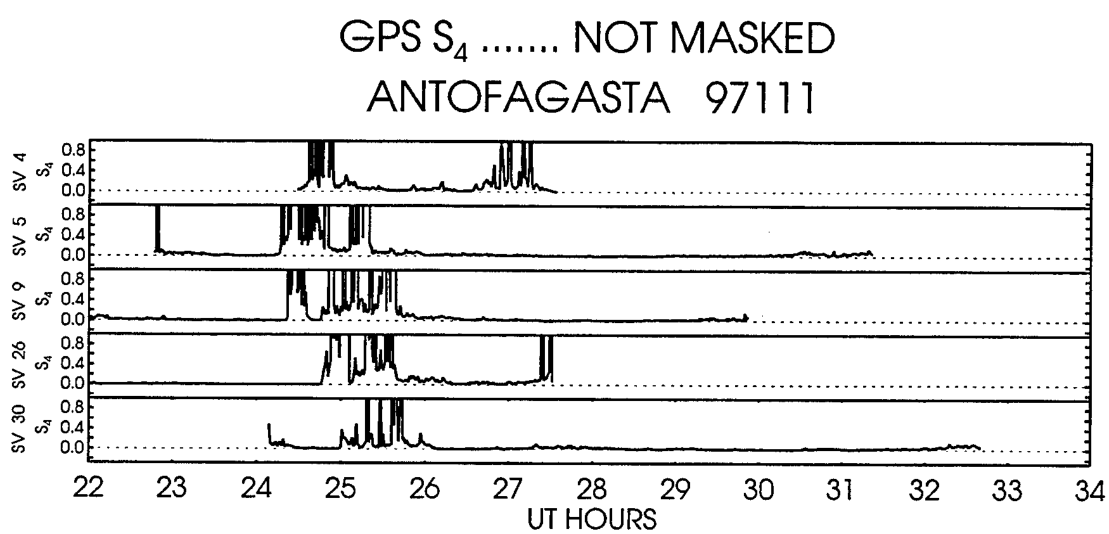

Figure 11. GPS S_4 values recorded for selected satellites over Antofagasta on the evening of 21 April 1997 (97111). A severe signal disruption was seen by each of these satellites.

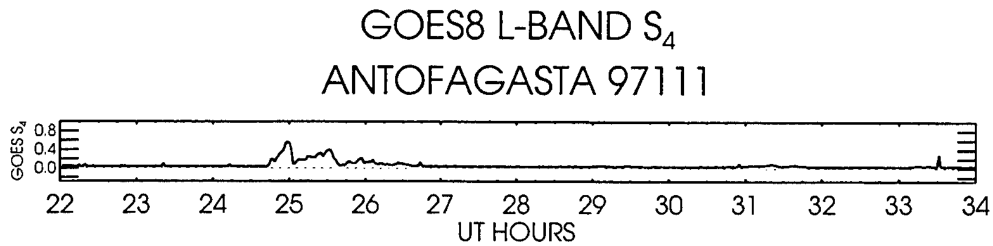

Figure 12. L-band S_4 values on the GOES8 link to a receiver at Antofagasta, Chile on the evening of 21 April 1997 (97111). The maximum scintillation levels seen here are just over 0.4.

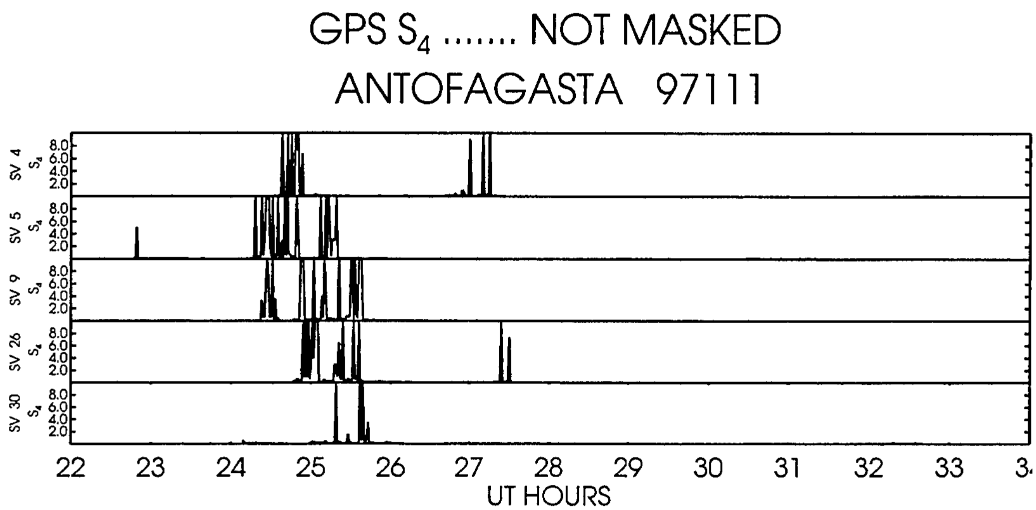

Figure 13. Similar to Figure 11, GPS S_4 values are shown for selected satellites over Antofagasta on the evening of 21 April 1997 (97111). The y-axis (S_4) scale has been increased to demonstrate the extremely large S_4 values being recorded.

Figure 13 contains the same data as Figure 11, with the S_4 scale increased to a maximum of 10.0. Notice that the S_4 values exceed this maximum for each satellite included. In order to correctly distinguish levels of L-band scintillation, this must be corrected. The 60-second phase sigma appears to demonstrate a more consistent behavior than the S_4 values and therefore is currently being used in the first implementation of GPS data into SCINDA. This can be seen in Figure 14, where the GOES8 S_4 is plotted along with the GPS S_4, elevation angle, and 60-second phase sigma for selected satellites from the evening of 2 November 1997 (97306). The phase values during the scintillation events recorded here remain within the accepted range while the S_4 levels are off the scale.

GOES S_4 / GPS S_4, ELEVATION, & 60 SEC PHASE
ANTOFAGASTA 97306 : NOT MASKED

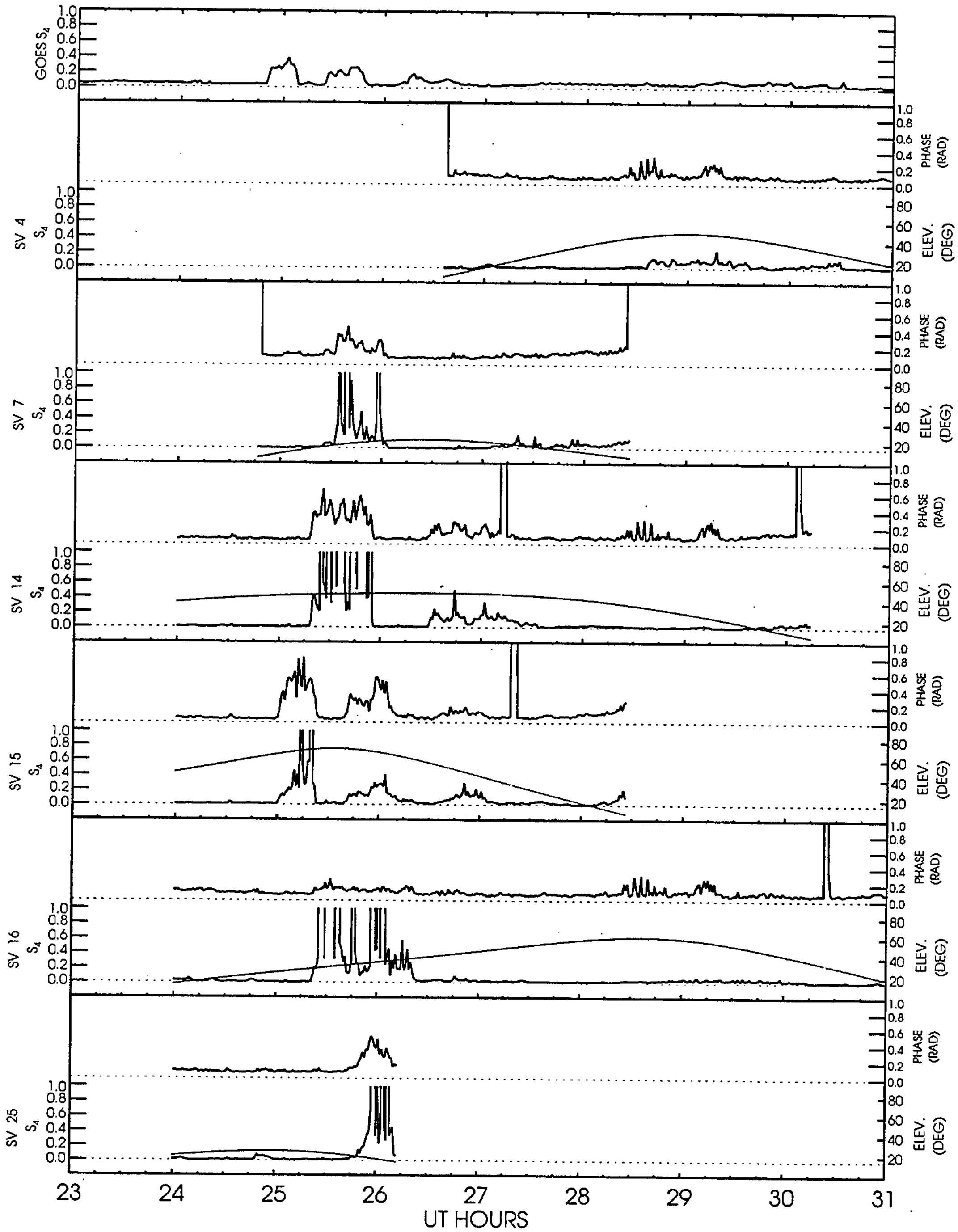

Figure 14. GOES8 and GPS measurements over Antofagasta for selected satellites on the evening of 2 November 1997 (97306). The S_4, 60-Second Phase Sigma, and elevation angles are plotted for each GPS satellite.

6. ANTENNA PATTERN CHARACTERIZATION

In order to prevent issuing false scintillation warnings, it is necessary to characterize the local antenna pattern at each site and disregard possible false scintillation observations. Careful examination of GPS S_4 summary plots reveal that certain satellites exhibit a repeating pattern of extremely high S_4 measurements in the same locations during each orbit. Examples of this were pointed out in the discussion of Figures 5, 6, 9, and 10. In order to characterize these measurements, calculations were made of the average S_4, carrier-to-noise, and 60-second phase sigma values while sorting the data, from both Ancón, Peru and Antofagasta, Chile, into one degree azimuth and elevation bins. In calculating these averages, it was necessary to disregard the extremely large S_4 or phase sigma values recorded by the NovAtel receivers. This was accomplished by limiting the data to phase sigma and S_4 values below 0.3.

An image of the average S_4 values in one degree azimuth and elevation bins measured at Antofagasta, Chile is shown in Figure 15.

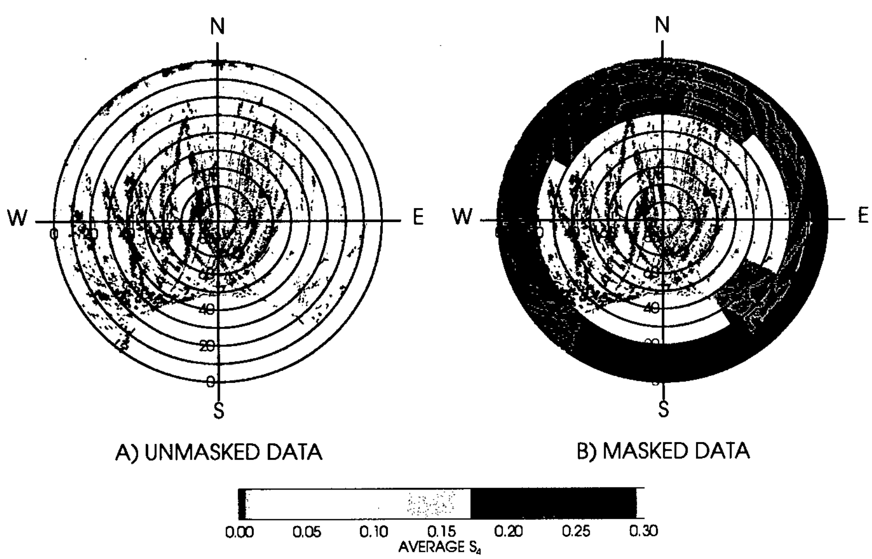

Figure 15. GPS average S_4 values in one degree azimuth and elevation bins from Antofagasta, Chile. S_4 values above 0.3 are not included in average calculations. Data was collected between 28 Oct 1996 (96302) and 13 June 1997 (97164) with copious data dropouts.

The data included here were collected between 28 October 1996 (96302) and 13 June 1997 (97164). Very little L-band scintillation was observed during this period of minimum solar activity. Comparing the unmasked image in Figure 15a with the color scale legend at the bottom of the figure, it is apparent that satellites below 20° elevation, particularly to the north-northwest, and satellites to the southeast of the station below 40° routinely experience location dependent signal disruptions.

To guard against false scintillation warnings caused by the persistent interference, site specific masks are generated to effectively screen data in the persistent anomalous regions. For example, the S_4 data displayed in Figure 15a suggests a mask as shown in Figure 15b. The black shaded regions in Figure 15b indicate masked areas. The data presented in Figure 9 from the evening of 23 November 1996 (96328) was displayed without applying a mask. The same data is plotted again in Figure 16, this time making use of the mask in Figure 15b which was specifically designed for the antenna configuration at Antofagasta, Chile. With all data in the masked regions being plotted with a value of -0.2, the large S_4 values seen in Figure 9 for GPS satellites 18, 19, and 27 are no longer seen. Figure 17, created with the GPS tracking software discussed in Section 4, shows that both SV 19 and SV 27 pass directly through the anomalous region to the southeast shown in Figure 15a.

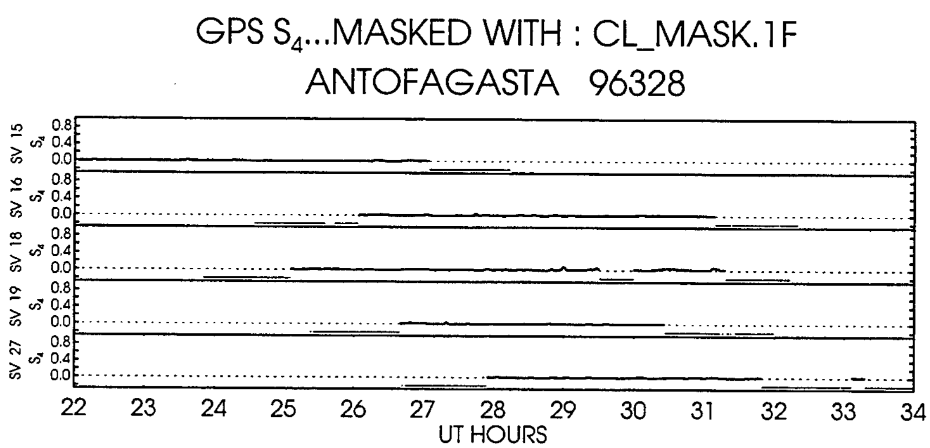

Figure 16. Similar to Figure 9, GPS S_4 values are shown for selected satellites over Antofagasta, Chile on the evening of 21 April 1997 (97111). For this plot, the mask shown in Figure 15b has been applied, eliminating possible multipath effects. All data within masked regions are plotted with values of -0.2.

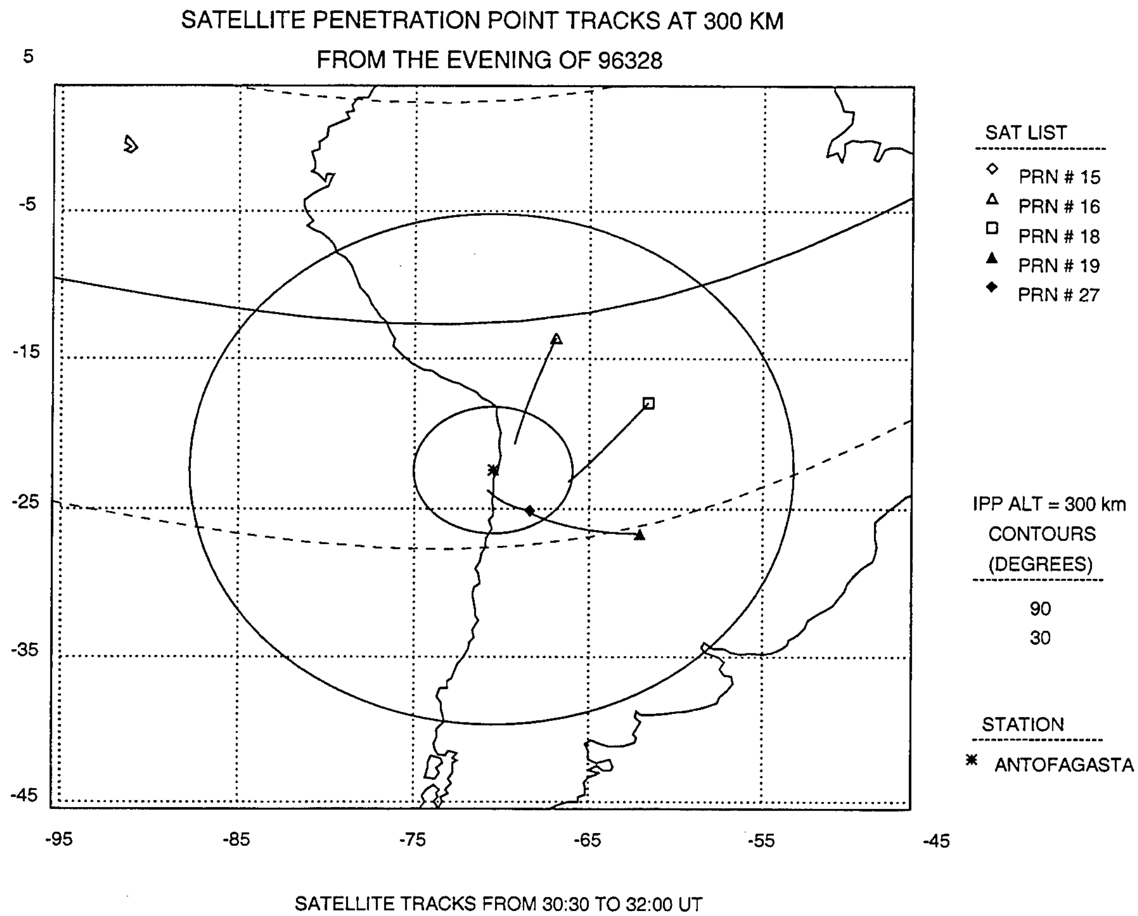

Figure 17. GPS ionospheric penetration point tracks from the evening of 23 November 1996 (96328). Notice that SV 27, at 32:00 UT, is entering the same region occupied by SV 19 at 30:30 UT. It is near this location, to the Southeast of Antofagasta, where severe S_4 disturbances are routinely seen.

Figures 18a and 18b are similar to those shown in Figure 15 but for the station at Ancón rather than Antofagasta. The importance of site specific masks is seen in the differences between the black regions (masks) of Figures 18 and 15. It should also be pointed out that these masks are subject to change over time due to antenna position or locations of adjacent antenna or other structures. This was taken into consideration by implementing a version control on the mask files.

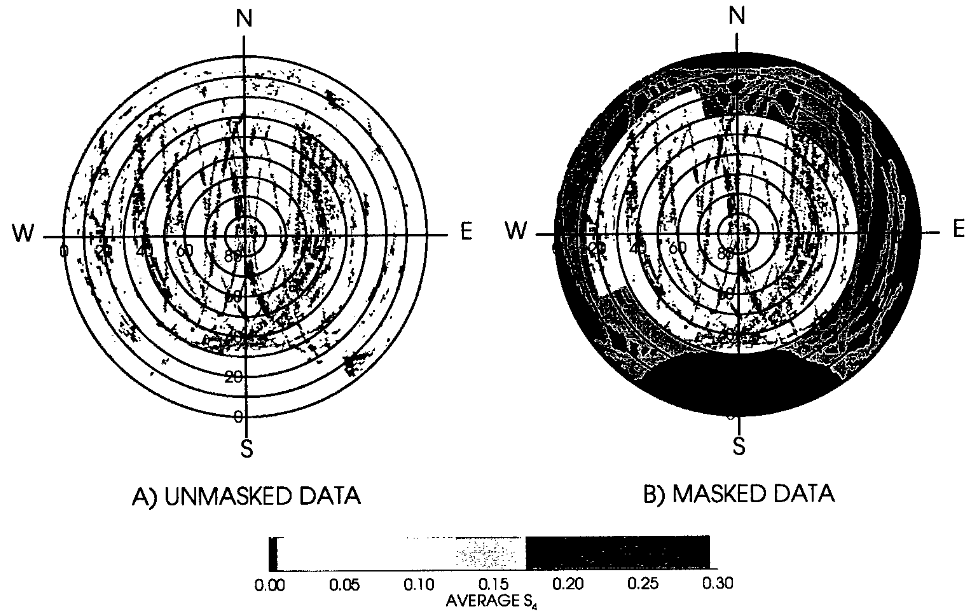

Figure 18. GPS average S_4 values in one degree azimuth and elevation bins from Ancón, Peru. S_4 values above 0.3 are not included in average calculations. Data was collected between 14 November 1996 (96320) and 24 January 1997 (97024) with multiple data dropouts.

The masks files displayed here were created with specially designed FORTRAN code. The elevation and azimuth regions to be masked were entered resulting in a file consisting of 1's and 0's for each one degree elevation and azimuth bin. A '0' signifies data within a multipath region to be masked while a '1' bin indicates data which may be accepted and used in issuing scintillation warnings. A separate program reads the raw GPS scintillation data and the mask file, creating a nightly masked data file to be used in various plotting routines.

As previously discussed in Section 5, the extremely high S_4 values recorded by the current system, even during moderate scintillation, have made it necessary to make use of the 60-second phase sigma rather than S_4 values for the current operational L-band features in SCINDA. Because of this, a new phase mask was designed for operational use which is slightly different than the S_4 mask shown here (See Appendix).

7. SUMMARY

SCINDA, a real-time UHF and L-band scintillation warning system, has been developed for the Air Force as a prototype providing support for military operations. The addition of GPS data to the system greatly enhances the detection and characterization of L-band scintillation. This report detailed investigations into several issues involved with the validation of the GPS data recorded by the NovAtel receivers. Mapping the GPS ionospheric penetration points, colored by their scintillation levels as calculated from the raw power data, indicates a very strong agreement with 6300 nm All-Sky airglow depletions over Agua Verde. Several problems have been noticed, however, in the GPS S_4 measurements. In comparisons with GOES8 L-band data, the GPS S_4 values are much too high. This same problem is not seen in the phase sigma data which are currently being used in SCINDA in place of S_4. Masking the GPS data in order to avoid false scintillation warnings due to suspected multipath effects is an important issue. The process used in developing these site specific masks, along with examples of their effects on the data, were presented in this report.

8. REFERENCES

Aarons, J. and Sa. Basu, "Scintillation on transionospheric radio signals", *Handbook of Geophysics and the Space Environment,* A. S. Jursa, Editor, AF Geophysics Laboratory, AF Systems Command, USAF, pp. 10-72., AFGL-TR-85-0315, ADA167000, 1985.

Beach, T. L., M. C. Kelly, P. M. Kintner, and C. A. Miller, Total electron content variations due to nonclassical traveling ionospheric disturbances: Theory and Global Positioning System observations, *J. Geophys. Res., 102,* 7279-7292, 1997.

Bishop, G., Sa. Basu, E. Holland, and J. Secan, Impacts of ionospheric fading on GSP navigation integrity, in *Proceedings of ION GPS-94,* pp. 557-566, Inst. of Navig., Alexandria, Va., 1994.

Calais, E. and B. Minster, GPS detection of ionospheric perturbations following a Space Shuttle ascent, *Geophys. Res. Letters, 23, 1996.*

Ho, C. M., A. J. Mannucci, U. J. Lindqwister, X. Pi and B. T. Tsurutani, Global ionosphere perturbations monitored by the worldwide GPS network. *Geophys. Res. Letters, 23,* 3219-3222, 1996.

Houminer, Z. and H. Soicher, Improved short-term predictions of f_oF_2 using GPS time delay measurements, *Radio Science, 31*, 1099-1108, 1996.

Hua, Quyen, Ionospheric scintillation monitor for C^3I, *PAQ-TR-10012,* Paq Communications, Milpitias, CA, 1996.

McNeil, W. J., A. R. Long and M. J. Kendra, Detection and characterization of equatorial scintillation for real-time operational support, *PL-TR-97-2059 Scientific Report #12,* Radex, Bedford, MA, 1997, ADA329175.

Pi, X., A. J. Mannucci, U. J. Lindqwister, and C. M. Ho, Monitoring of global ionospheric irregularities using the worldwide GPS network, *Geophys. Res. Letters., 24,* 2283-2286, 1997.

Weber, E. J., Sa. Basu, T. W. Bullet, C. Valladares, G. Bishop, K. Groves, H. Kuenzler, P. Ning, P. J. Sultan, R. E. Sheehan, and J. Araya, Equatorial plasma depletion precursor signatures and onset observed at 11° South of the magnetic equator, *J. Geophys. Res.,101*, 26829,1996.

APPENDIX A. CURRENT GPS SITE MASKS FOR ANCÓN AND ANTOFAGASTA

A.1 INDIVIDUAL MASKS

The current masks for Ancón, Peru and Antofagasta, Chile are shown below.

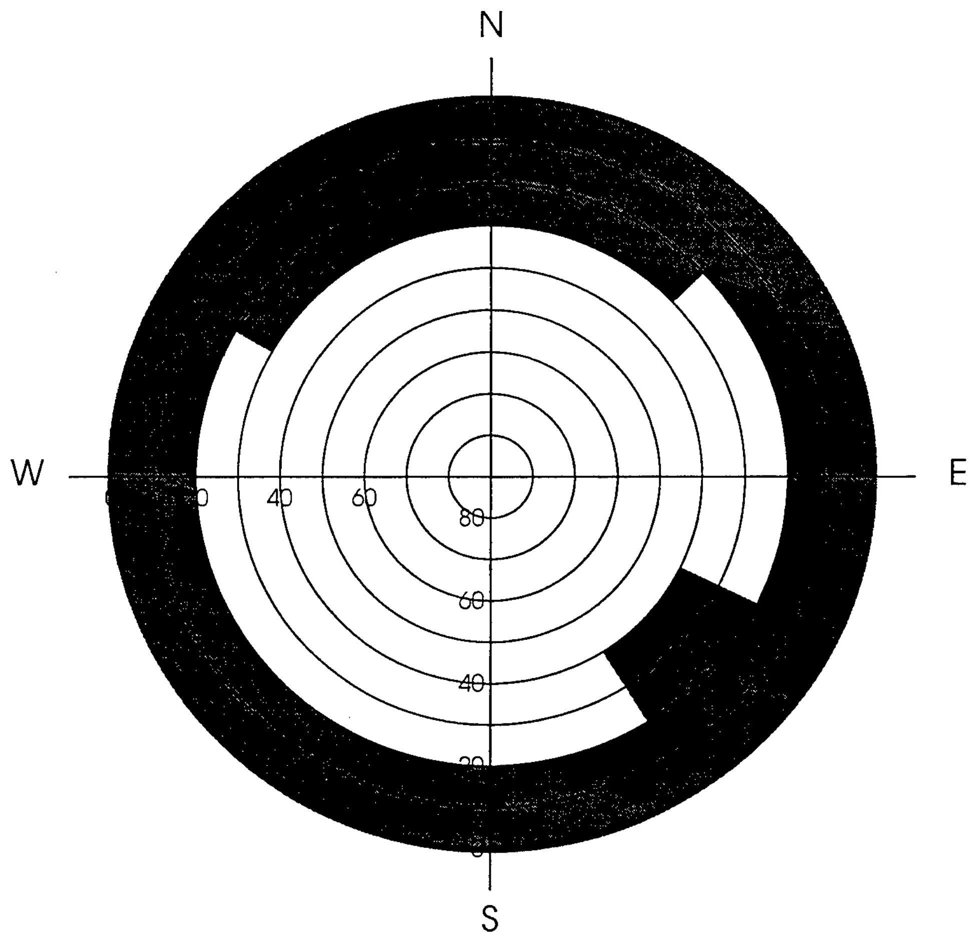

Figure A-1. CL_MASK.1F: The current GPS mask developed for Antofagasta, Chile from the S_4 data collected from 28 October 1996 (96302) to 13 June 1997 (97164).

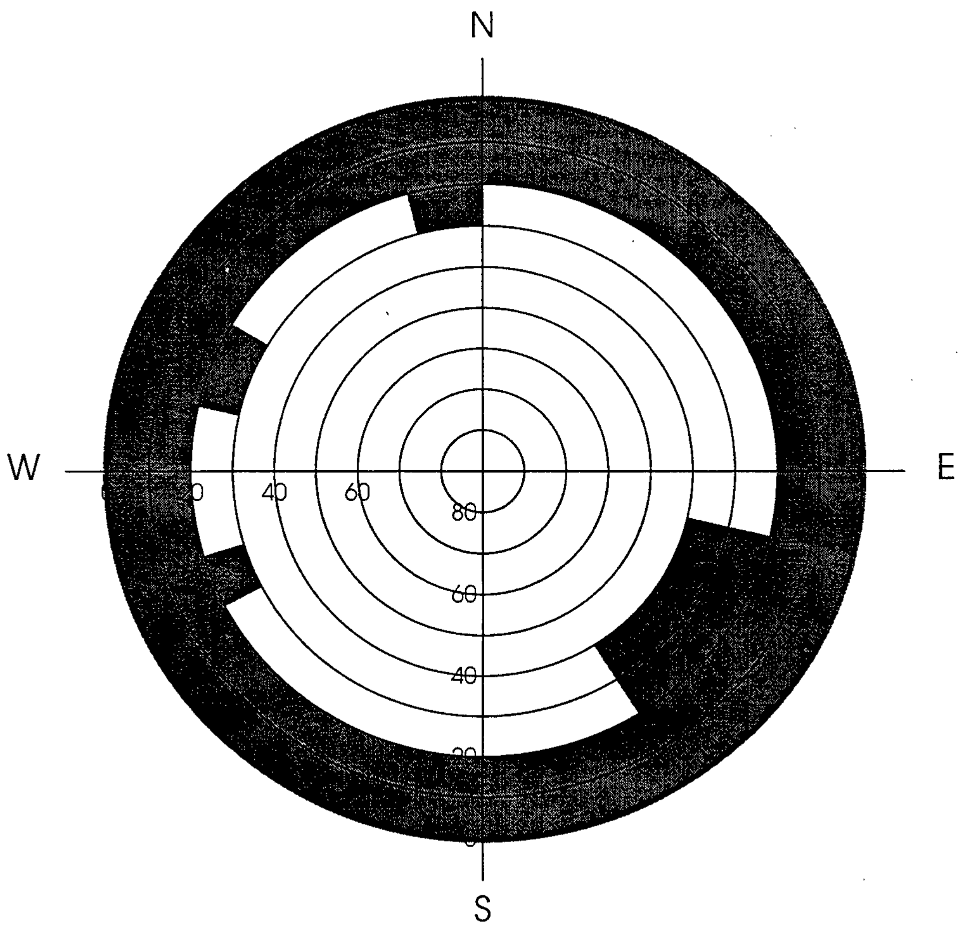

Figure A-2. CL_MASK_PHASE.1A: The current GPS mask developed for Antofagasta, Chile from the 60-second phase sigma data collected from 28 October 1996 (96302) to 13 June 1997 (97164).

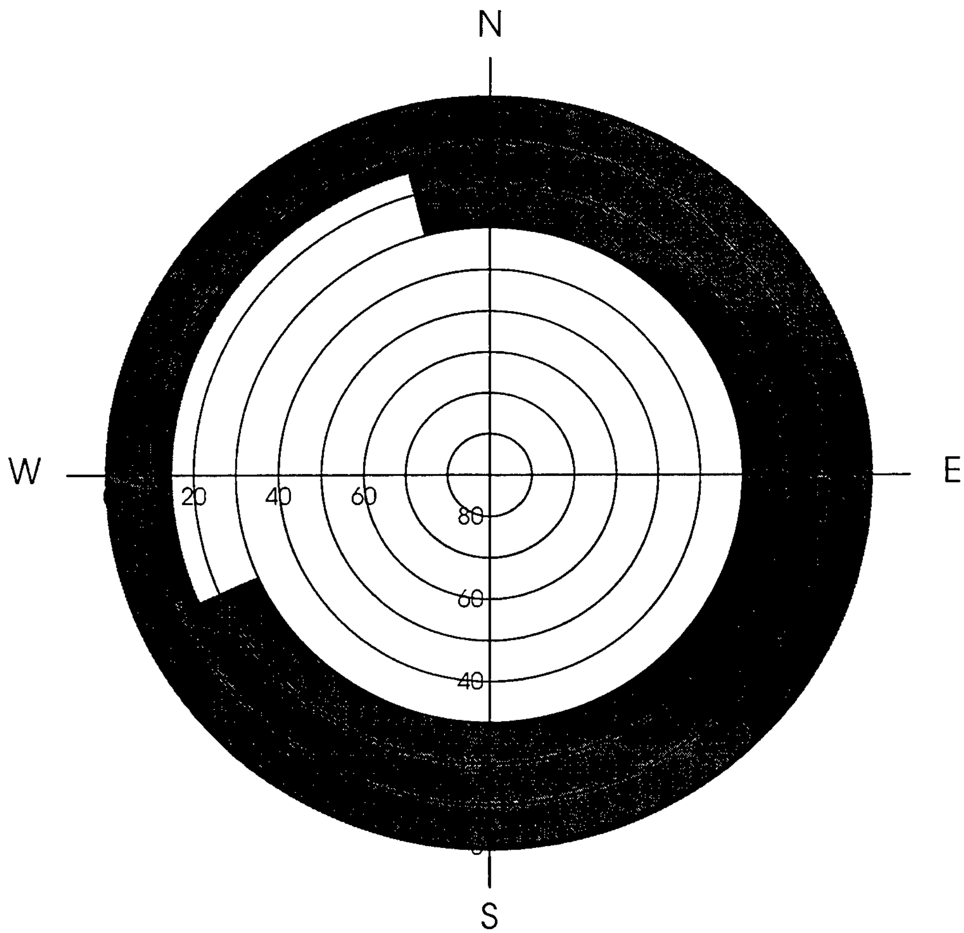

Figure A-3. PR_MASK.1A: The current GPS mask developed for Ancón, Peru from the 60-second phase sigma data collected from 14 November 1996 (96320) to 24 January 1997 (97024). The phase data from Ancón has not been analyzed at this time.

A.2 MASK FILE FORMAT

The following is a truncated example of a GPS site mask produced by the FORTRAN routine 'mk_mask.f.' The example shown is the file CL_MASK.1F shown in Figure A-1 and created from the S_4 values recorded at Antofagasta, Chile from 28 October 1996 (96302) to 13 June 1997 (97164). A description of the mask is included in the header information of the file.

```
25   ---- NUMBER OF HEADER RECORDS TO SKIP
 CL_MASK.1F   WAS GENERATED BY mk_mask.f
 A 1 OR 0 IS ASSIGNED TO EACH AZIMUTH AND ELEVATION BIN.
 EACH 0 BIN IS TO BE MASKED.

 THIS FILE WAS MADE WITH THE FOLLOWING INPUTS :

   > OVERALL CUTOFF AT 20 DEGREES ELEVATION.
   > PLUS  3 ADDITIONAL REGION(S) AT ....

   > AZIMUTH   = 116 TO 147 DEGREES
   > ELEVATION = BELOW 40 DEGREES

   > AZIMUTH   = 300 TO 359 DEGREES
   > ELEVATION = BELOW 30 DEGREES

   > AZIMUTH   =   0 TO  45 DEGREES
   > ELEVATION = BELOW 30 DEGREES


 THE X-AXIS IS FOR ELEVATION ANGLES FROM 0 TO 90 DEGREES.
 THE Y-AXIS (INDENT 5 SPACES) IS FOR AZIMUTH ANGLES FROM 0 TO 359 DEGREES.
-----------------------------------------------------------------------------

     0123456789012345678901234567890123456789012345678901234567890123456789012345678901234567890

   0 0000000000000000000000000000001111111111111111111111111111111111111111111111111111111111111
   1 0000000000000000000000000000001111111111111111111111111111111111111111111111111111111111111
   2 0000000000000000000000000000001111111111111111111111111111111111111111111111111111111111111
   3 0000000000000000000000000000001111111111111111111111111111111111111111111111111111111111111
   4 0000000000000000000000000000001111111111111111111111111111111111111111111111111111111111111
   5 0000000000000000000000000000001111111111111111111111111111111111111111111111111111111111111
   6 0000000000000000000000000000001111111111111111111111111111111111111111111111111111111111111
   7 0000000000000000000000000000001111111111111111111111111111111111111111111111111111111111111
   8 0000000000000000000000000000001111111111111111111111111111111111111111111111111111111111111
   :
   :
   :
 355 0000000000000000000000000000001111111111111111111111111111111111111111111111111111111111111
 356 0000000000000000000000000000001111111111111111111111111111111111111111111111111111111111111
 357 0000000000000000000000000000001111111111111111111111111111111111111111111111111111111111111
 358 0000000000000000000000000000001111111111111111111111111111111111111111111111111111111111111
 359 0000000000000000000000000000001111111111111111111111111111111111111111111111111111111111111
```